

RESEARCH

Open Access



Synergistic effect of human uterine cervical mesenchymal stem cell secretome and paclitaxel on triple negative breast cancer

Noemi Eiro^{1*} , Maria Fraile¹, Sara Escudero-Cernuda², Juan Sendon-Lago³, Luis O. Gonzalez¹, Maria Luisa Fernandez-Sánchez² and Francisco J. Vizoso^{1*} 

Abstract

Background Triple-negative breast cancer (TNBC) is the most lethal subtype of breast cancer and, despite its adverse effects, chemotherapy is the standard systemic treatment option for TNBC. Since, it is of utmost importance to consider the combination of different agents to achieve greater efficacy and curability potential, MSC secretome is a possible innovative alternative.

Methods In the present study, we proposed to investigate the anti-tumor effect of the combination of a chemical agent (paclitaxel) with a complex biological product, secretome derived from human Uterine Cervical Stem cells (CM-hUCESC) in TNBC.

Results The combination of paclitaxel and CM-hUCESC decreased cell proliferation and invasiveness of tumor cells and induced apoptosis in vitro (MDA-MB-231 and/or primary tumor cells). The anti-tumor effect was confirmed in a mouse tumor xenograft model showing that the combination of both products has a significant effect in reducing tumor growth. Also, pre-conditioning hUCESC with a sub-lethal dose of paclitaxel enhances the effect of its secretome and in combination with paclitaxel reduced significantly tumor growth and even allows to diminish the dose of paclitaxel in vivo. This effect is in part due to the action of extracellular vesicles (EVs) derived from CM-hUCESC and soluble factors, such as TIMP-1 and – 2.

Conclusions In conclusion, our data demonstrate the synergistic effect of the combination of CM-hUCESC with paclitaxel on TNBC and opens an opportunity to reduce the dose of the chemotherapeutic agents, which may decrease chemotherapy-related toxicity.

Keywords Secretome, Conditioned medium, Mesenchymal stem cells, hUCESC, Breast cancer, Chemotherapy

*Correspondence:

Noemi Eiro

noemi.eiro@hospitaldejove.com

Francisco J. Vizoso

investigacion@hospitaldejove.com

¹Research Unit, Hospital de Jove Foundation, Gijón, Spain

²Department of Physical and Analytical Chemistry, University of Oviedo,

Oviedo, Spain

³Experimental Biomedicine Centre (CEBEGA), University of Santiago de

Compostela, Santiago de Compostela, Spain



© The Author(s) 2024. **Open Access** This article is licensed under a Creative Commons Attribution 4.0 International License, which permits use, sharing, adaptation, distribution and reproduction in any medium or format, as long as you give appropriate credit to the original author(s) and the source, provide a link to the Creative Commons licence, and indicate if changes were made. The images or other third party material in this article are included in the article's Creative Commons licence, unless indicated otherwise in a credit line to the material. If material is not included in the article's Creative Commons licence and your intended use is not permitted by statutory regulation or exceeds the permitted use, you will need to obtain permission directly from the copyright holder. To view a copy of this licence, visit <http://creativecommons.org/licenses/by/4.0/>. The Creative Commons Public Domain Dedication waiver (<http://creativecommons.org/publicdomain/zero/1.0/>) applies to the data made available in this article, unless otherwise stated in a credit line to the data.

Background

The history of breast cancer dates back to 3,000–2,500 BC, the approximate date of the Edwin Smith papyrus [1], the oldest known medical document in the world, which contains the first written description of cancer. Fifteen centuries later (1,500 BC), in the Ebers papyrus, breast cancer with axillary metastasis was described for the first time, evoking the possibility of treatment by surgery, drugs or ignition. Cancer treatment was dominated by surgery and radiotherapy until the mid-1960s [2]. It was at that time, as part of a public programme to identify new anti-tumor compounds in the United States, that samples of Pacific yew (*Taxus brevifolia*) bark were found to exhibit potent cytotoxic activity (1964); paclitaxel was subsequently identified as the active ingredient of the extract [3]. Despite the development of new therapeutic modalities, chemotherapy remains the most widely used antineoplastic therapy in advanced breast cancer due to its high efficacy and despite its adverse effects [4–6].

Among breast cancer molecular subtypes, triple-negative breast cancer (TNBC), defined by the lack of estrogen (ER), progesterone (PR) and human epidermal growth factor receptor 2 (HER-2) expression, is the most lethal subtype of breast cancer with a 5-year mortality of about 40% [7–9]. Currently, chemotherapy is the standard systemic treatment option for TNBC. So, we are treating an old disease using an old therapy. Since, it is of utmost importance to consider the combination of different agents to achieve greater efficacy and curability potential [4]. In this sense, immunotherapy, one of the most significant advances in oncology, introduce biologic agents like monoclonal antibodies (atezolizumab) targeting PD-1 ligand (PD-L1), for example, in TNBC management [10, 11].

A possible innovative alternative could be the use of mesenchymal stem cells (MSC), defined as regenerative undifferentiated cells capable of being differentiated into various cell types [12]. MSC display a wide repertory of paracrine functions due to their secretion of a wide range of soluble factors, such as cytokines or growth factors, and extracellular vesicles. For all of this, MSC have aroused great interest due to their regenerative, anti-inflammatory, immunoregulatory, anti-oxidative stress, anti-fibrotic or anti-microbial properties [13]. Recent studies also show that MSC suppressing tumor growth by inhibiting tumor cell proliferation and inducing apoptosis in cancer cells [14]. Consequently, application strategies based on MSC were recently considered in TNBC [15]. In this regard, we described a new type of mesenchymal stem cell, called human Uterine Cervical Stem Cells (hUCESC), which are obtained from the transitional zone of the cervix of healthy women [16]. The method for obtaining hUCESC (Pap cervical smear or hysterectomy) is much less invasive and painful than those used

to obtain other MSC (from the bone marrow or adipose tissue). In addition, hUCESC can be isolated in high quantities, and have a high proliferative rate, making it possible to quickly obtain a huge amount of stem cells or conditioned medium for research and clinical use [16]. Our previous results showed that the secretome or conditioned medium of hUCESC (CM-hUCESC) has a specific anti-tumor effect on proliferation, apoptosis, and invasion of aggressive TNBC cell line MDA-MB-231 and primary mammary carcinoma cultures in vitro [16, 17]. These anti-tumor actions differ from those described for other mesenchymal stem cells [18–20] and may be due, in part, to the fact that CM-hUCESC has higher levels of factors with recognised anti-tumor effects, such as LIGHT (or TNFSF14), Fms-related tyrosine kinase 3 ligand (FLT-3 ligand), interferon gamma-inducible protein-10 (IP-10) and latency-associated protein, compared with CM from adipose-derived mesenchymal stem cells, for example [16].

Based on these data, we have proposed to study the anti-tumor effect of the combination of a chemical agent (paclitaxel) with a complex biological agent (CM-hUCESC) in TNBC.

Materials and methods

Primary tumors and breast cancer cell line culture

Primary cell cultures of breast tumors were obtained as previously reported [21, 22]. The estrogen-independent human breast cancer-derived cell line MDA-MB-231 were obtained from the American Type Culture Collection (ATCC, Rockville, MD, USA). MDA-MB-231 cells and primary cells were cultured in DMEM-F12 (Lonza, Visp, Switzerland) supplemented with 10% Fetal Bovine Serum (FBS) (Corning) and 1% penicillin-streptomycin solution (Gibco, Paisley, UK).

Conditioned medium production

hUCESC were obtained as previously described [16]. Conditioned medium from hUCESC was obtained from 80% cell culture confluence. Afterwards, the cells were washed three times in PBS, and cultured in DMEM-F12 without FBS and antibiotics. After 48 h, the medium was centrifuged for 5 min at 400 g, the supernatant was collected and stored at -80°C. For the in vivo studies, the CM-hUCESC was lyophilized and then stored at -80 °C until used and resuspended just before use in the half volume of deionized distilled water (ddH₂O) to obtain the concentrated CM-hUCESC (2X).

For the production of CM-hUCESC in presence of chemotherapy (CM-hUCESC_{chemo}), hUCESC were incubated in presence of a sub-lethal concentration of paclitaxel (10 μM) (Teva Pharma) during 24 h [23]. Afterwards, the cells were washed, and the conditioned medium was produced as previously described.

Proliferation assay

To determine the effect of the combination of CM-hUCESC or CM-hUCESC_{chemo} with paclitaxel (1 μ M, 3 μ M and 5 μ M) on the proliferation capacity of the aggressive breast cancer cell line MDA-MB-231 and breast cancer primary tumors. Cells were seeded in 96-well plates in DMEM-F12 supplemented with 10% FBS and 1% penicillin-streptomycin. After 24 h, the media was removed and cells were treated with 100 μ L per well of CM-hUCESC or CM-hUCESC_{chemo} with or without paclitaxel, using DMEM-F12 medium as a control, and cultured for 48 h. Finally, 10 μ L of the WST-1 proliferation reagent (Roche) was added and incubated for 4 h at 37 °C and 5% CO₂. Proliferation was quantified measuring the absorbance at 450 nm and subtracting the absorbance value at 655 nm.

Cell cycle and apoptosis assay

Breast cancer cells were seeded in complete medium, washed, and then treated for 24 h in the following conditions: control (DMEM-F12), CM-hUCESC, chemotherapy (paclitaxel 1 μ M) and a combination of CM-hUCESC and chemotherapy. Forty-eight hours later, cells were harvested, fixed with ethanol (70%), washed and stained with propidium iodide (50 μ g/ml) for 1 h in darkness and cell cycle was analysed by flow cytometry.

Apoptosis analyses were performed using Annexin V-FITC. Briefly, cells were harvested, washed, and resuspended in 1X binding buffer. 5 μ L of FITC-Annexin V was added and incubated for 15 min at room temperature in darkness. Finally, 400 μ L of 1X binding buffer was added to each tube and analysed.

Cell invasion assay

Assays were performed in BD BioCoat Matrigel invasion chambers according to the manufacturer's instructions (BD Biosciences, Madrid, Spain). MDA-MB-231 cells were seeded (50,000 cells) into the upper chamber in DMEM-F12 (control), paclitaxel (1 μ M), CM-hUCESC, CM-hUCESC_{chemo} or combination of paclitaxel+CM-hUCESC/CM-hUCESC_{chemo}. After incubation for 48 h, cells that had migrated to the lower surface of the filters were fixed in methanol, stained using crystal violet, visualized and counted. Values for cell migration or invasion were expressed as the mean number of cells per microscopic field over four fields per one filter for duplicate experiments.

Immunoprecipitation (IP) and Western blot (WB)

As described previously, protein A/G PLUS-Agarose (70 μ L, sc-2003, Santa Cruz Biotechnology, Dallas, USA) and anti-TIMP-1 antibody (5 μ L, sc-365,905, Santa Cruz Biotechnology) or anti-TIMP-2 antibody (5 μ L, sc-365,671, Santa Cruz Biotechnology), or IgG1 mouse

(5 μ L, used as IP control, sc-3877, Santa Cruz Biotechnology) were mixed with 8 ml of CM-hUCESC and incubated overnight at 4 °C in orbital shaking. Then, samples were centrifuged and the supernatant used for functional assays [24].

The precipitate was used to evaluate TIMP-1 and TIMP-2 IP by Western blot. Briefly, after 12% SDS-PAGE electrophoresis, proteins were transferred to a PVDF membrane, blocked, and immunolabeled with TIMP-2 primary antibody (1/200, Thermo-Scientific, Rockford, USA) and second antibody (anti-mouse HRP, 1/3000, Sigma). Signal was detected with the SuperSignal West Pico Plus (Thermo Scientific, Rockford, USA), and visualized by placing the blot in contact with standard X-ray film.

Isolation and characterization of CM-hUCESC_{chemo} extracellular vesicles

Isolation of extracellular vesicles (EVs) was performed by differential ultracentrifugation, as described previously [25]. The pellet obtained by ultracentrifugation at 100,000 g for 70 min corresponding to the fraction containing the EVs was resuspended in 0.1 μ m filtered PBS with sucrose at 1% (Sigma-Aldrich). The presence of EVs in the sample was detected by Transmission Electron Microscopy (TEM) JEM-1011 (JEOL, Japan) at 100 kV with a previous fixing with 2% paraformaldehyde and dyed with 2% phosphotungstic acid. The EVs and Taxol-encapsulated EVs were characterized by a Pierce™ bicinchoninic acid assay kit (Thermo Fisher Scientific, USA) for total protein quantification. The size distribution and particle concentration were determined by Nanoparticle Track Analysis (NTA) Nanosight LM10 (Malvern Panalytical, United Kingdom).

EVs were characterized by flow cytometry using specific antibodies: anti-CD9 antibody (FITC) (Abcam, United Kingdom), anti-CD63 (APC) (Bio-Rad, USA) and anti-CD81 antibody (PE) (Bio-Rad, USA). Also, the Molecular Probes™ CellTrace™ Calcein Violet, AM (Invitrogen, USA) was used to ensure EVs integrity. The fluorescence was monitored by a Cytoflex S Flow Cytometer using a Violet Laser (405 nm) and its light Side Scattering (SSCviolet).

Determination of paclitaxel by HPLC-ESI-Q-TOF

For paclitaxel determination, EVs, CM-hUCESC_{chemo} and hUCESC cells were lysed as previously described [23]. The lysate were dried by speed vacuum (Concentrator 5301 Eppendorf), resuspended in the chromatographic initial phase and spiked with Docetaxel at 200 ng/mL as Internal Standard and injected into the HPLC (Dionex Ultimate 3000). The chromatographic separation was performed with an InfinityLab Poroshell 120 EC-C18 column using ultrapure water (LabWater, Purelab Flex

system ELGA, UK) as phase A and acetonitrile (Fischer Scientific, USA) as phase B, both with formic acid at 0.1% (Acros Organics, Germany). The chromatographic gradient was performed at 0.2 mL/min (0 min–40% B, 2 min–40% B, 10 min–60% B). Paclitaxel was detected by an ESI-QTOF spectrometer (Bruker Impact II model) with the following settings: capillary voltage 3500 V, dry gas at 6 L/min, dry temperature of 250°C, mass range (m/z) between 50 and 1500 and spectra rate of 1.00 Hz.

Animal studies

Six weeks old female NMRI Fox1 nu/nu mice were used for xenografting studies. Twenty-eight mice (7 per group) were injected into the mammary fat pads with 2.5×10^6 MDA-MB-231-luc- cells in matrigel. Ten days after cell injection, the mice were treated until day thirty: group 1 (control): DMEM-F12 culture medium+saline solution; group 2: CM-hUCESC (2X) intraperitoneally (200 μ l) 3 times/week; group 3: paclitaxel 10 mg/kg intraperitoneally once/week and group 4: CM-hUCESC (2X) intraperitoneally (3 times/week)+paclitaxel 10 mg/kg intraperitoneally (once per week). Tumor growth was monitored by luminescence, after luciferin injection (150 mg/kg), mice were anesthetized using 2.5% isoflurane and imaged using the In Vivo Imaging System (IVIS, Caliper Life Sciences, Alameda, CA, USA) at day 0, 7, 14, 21 and 30. An intensity map was obtained using the Living Image software (Caliper Life Sciences). The software uses a color-based scale to represent the intensity of each pixel (from blue representing low to red representing high).

To investigate the effect of CM-hUCESC_{chemo}, a similar study was conducted as follows: group 1 (control) ($n=4$): DMEM-F12 culture medium+saline solution; group 2 ($n=7$): CM-hUCESC_{chemo} intraperitoneally (200 μ l) 3 times/week; group 3 ($n=7$): paclitaxel 5 mg/kg intraperitoneally once/week and group 4 ($n=7$): CM-hUCESC_{chemo} intraperitoneally (3 times/week)+paclitaxel 5 mg/kg intraperitoneally (once per week).

All animals were euthanized by carbon dioxide inhalation. The manuscript reporting adheres to the ARRIVE (Animal Research: Reporting of In Vivo Experiments) 2.0 guidelines.

Statistical analysis

Data analysis and statistics (t-tests, ANOVA, Kruskal-Wallis) were conducted with PASW Statistics 18 (San Diego, CA, USA) and a p value <0.05 was considered statistically significant. We have also calculated the adjusted p-values using the Benjamini-Hochberg procedure, also known as the False Discovery Rate (FDR) procedure, used to control the expected proportion of false discoveries.

Results

Synergistic effect of CM-hUCESC in combination with paclitaxel on breast cancer cell proliferation

As shown in Fig. 1, MDA-MB-231 cells and primary breast cancer cells treated with CM-hUCESC and/or paclitaxel showed a significant inhibition of proliferation compared with the control (DMEM-F12). As expected, the higher the concentration of paclitaxel showed the greater inhibition of cell proliferation among paclitaxel treated cells. However, the combination of paclitaxel 1 μ M with CM-hUCESC significantly increased the inhibition of proliferation of MDA-MB-231 cells and primary tumors, showing a synergic effect ($p < 0.0001$, for both, adjusted p value = 0.0007, for both). In fact, the addition of CM-hUCESC to a low dose of paclitaxel showed similar or even superior proliferation inhibition to that exhibited with a higher concentration of paclitaxel; in this sense, cells treated with 1 μ M paclitaxel+CM-hUCESC showed a greater inhibition of cell proliferation to that shown by cells treated with 3 μ M paclitaxel+CM-hUCESC.

Effect of combination of CM-hUCESC and paclitaxel on cell cycle and apoptosis

Given that paclitaxel+CM-hUCESC significantly decreased proliferation of MDA-MB-231 cells, we next evaluated cell cycle and apoptosis as possible mediators. As shown in Fig. 2, cells treated with paclitaxel, CM-hUCESC or the combination paclitaxel+CM-hUCESC decreased their G0-G1 phase in relation to cells treated with control (DMEM-F12) but increased their G2-M phase in relation to control (Fig. 2A).

Treatment of MDA-MB-231 cells with paclitaxel+CM-hUCESC induced a decrease of live cells (Annexin-/PI-) compared with control, CM-hUCESC alone or paclitaxel alone and an increase of Annexin V+ / PI+ cells suggesting that the combination of both treatments induces late apoptosis (Fig. 2B).

Inhibition of breast cancer cell invasiveness by combining CM-hUCESC with paclitaxel

In order to evaluate the impact of the combination of both treatments on cell invasion capacity, we have carried out a functional study treating the breast cancer cell line MDA-MB-231 with DMEM-F12 (control), CM-hUCESC, paclitaxel (1 μ M) and the combination of paclitaxel+CM-hUCESC. As shown in Fig. 2C, CM-hUCESC significantly inhibited MDA-MB-231 cell invasion capacity (28%, $p < 0.0001$ compared with control (adjusted p value = 0.004)) but the inhibition of the invasion capacity is higher by paclitaxel (61%) ($p < 0.0001$ compared with CM-hUCESC, (adjusted p value = 0.004)). Although, the combination of both (paclitaxel+CM-hUCESC) showed the highest inhibition of breast cancer cell invasiveness

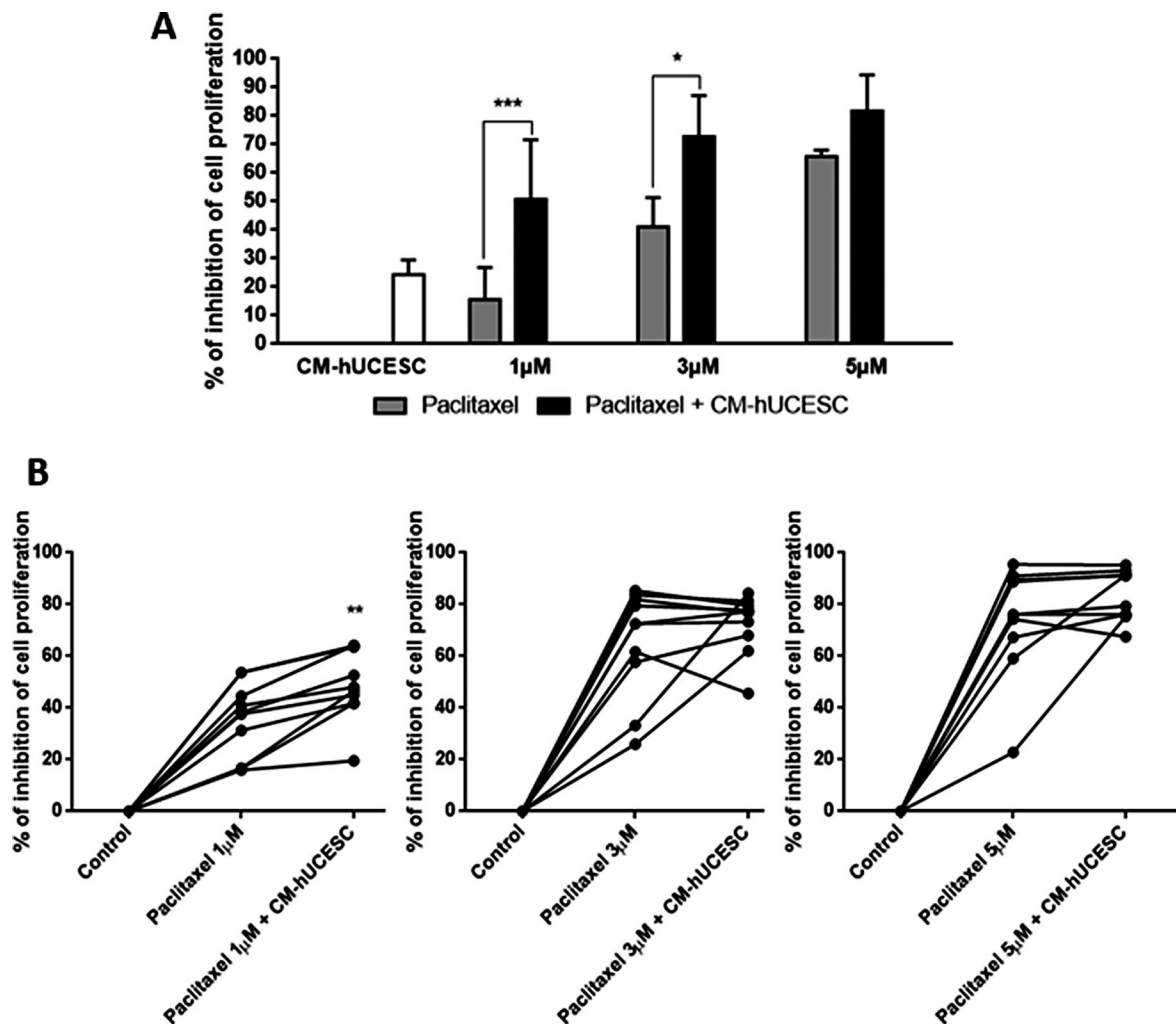


Fig. 1 (A) Relative proliferative capacity of MDA-MB-231 cells treated for 48 h with CM-hUCESC, paclitaxel (1 μ M, 3 μ M and 5 μ M) and the combination of paclitaxel (1 μ M, 3 μ M and 5 μ M) + CM-hUCESC. (B) Relative proliferative capacity of primary tumor cells from TNBC treated for 48 h with CM-hUCESC, paclitaxel (1 μ M, 3 μ M and 5 μ M) and the combination of paclitaxel (1 μ M, 3 μ M and 5 μ M) + CM-hUCESC. * $p < 0.05$, *** $p < 0.0001$

there was no significant difference compared with paclitaxel alone.

TIMP-1 and TIMP-2 mediate the anti-tumoral effect induced by CM-hUCESC

We have previously described that some factors secreted by mesenchymal stem cells could be responsible for their therapeutic effects [26] and that the tissue inhibitors of metalloproteinases TIMP-1 and -2 are present at high levels in CM-hUCESC [24]. To establish if TIMP-1 and -2 are involved in the anti-tumoral effect induced by CM-hUCESC, they were immunoprecipitated (IP) from the CM-hUCESC with specific antibodies. IgG IP was used as control. A Western blot was carried out demonstrate the immunoprecipitation of TIMP-2 (supplementary Fig. 1). In the case of TIMP-1 the molecular weight of the light chain of the anti-TIMP-1 antibody (25 kDa) used in the immunoprecipitation is close to the molecular

weight of the TIMP-1 protein (29 kDa). Due to the excess of the antibody use during the immunoprecipitation (to ensure that all TIMP-1 is immunoprecipitated) and the intensity of the band, this band masks the detection of any protein of interest with a molecular weight close to 25 kDa (data not shown). Then, a cell invasion assay was carried out with MDA-MB-231 cells treated with whole CM-hUCESC or without TIMP-1 and -2. Complete CM-hUCESC significantly decreased migration of cancer cell line as compared with control ($p < 0.0001$, adjusted p value = 0.0007) and with CM-hUCESC lacking TIMP-1 and -2 (IP TIMP-1/2) ($p = 0.004$, adjusted p value = 0.008) (Fig. 2D). Moreover, invasion of confluent MDA-MB-231 cells induced by CM-hUCESC lacking TIMP-1 and -2 was similar to that induced by control.

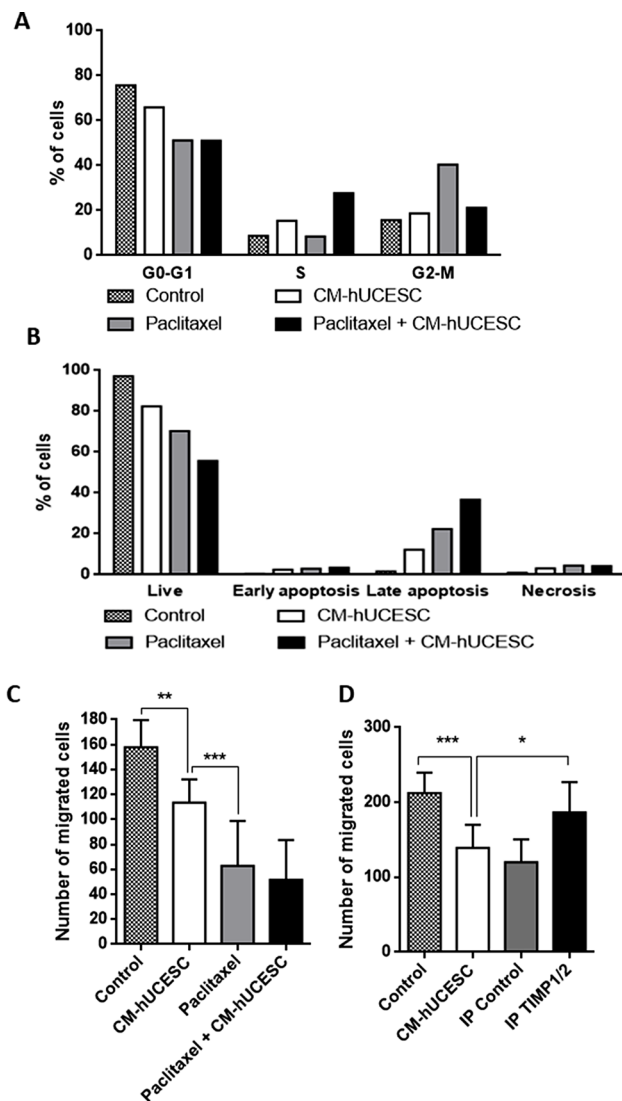


Fig. 2 (A) Cell cycle analysis of MDA-MB-231 cells treated for 48 h with control (DMEM-F12 without FBS), CM-hUCESC, paclitaxel (1 μ M) or the combination of paclitaxel (1 μ M)+CM-hUCESC, and then subjected to flow cytometry using propidium iodide (PI). Percentage of cells (mean + standard deviation) in each phase is shown. (B) Apoptosis was determined in MDA-MB-231 cells cultured for 48 h with control (DMEM-F12 without FBS), CM-hUCESC, paclitaxel (1 μ M) or the combination of paclitaxel (1 μ M)+CM-hUCESC, by flow cytometry using Annexin V/PI. Annexin V+/PI- and Annexin V+/PI+ indicated early and late apoptosis, respectively. (C) Invasive capacity of MDA-MB-231 cells treated for 48 h with control (DMEM-F12 without FBS), CM-hUCESC, paclitaxel (1 μ M) or the combination of paclitaxel (1 μ M)+CM-hUCESC in Matrigel invasion chambers. (D) Invasive capacity of MDA-MB-231 cells treated for 48 h with control (DMEM-F12 without FBS), CM-hUCESC, IgG IP and CM-hUCESC lacking TIMP-1 and -2 (IP TIMP-1/2) in Matrigel invasion chambers. Data represent the mean \pm SD. * p < 0.05; *** p < 0.0001

In vivo effect of combination of CM-hUCESC and paclitaxel

We have evaluated the effect of intraperitoneal administration of paclitaxel (10 mg/kg) and CM-hUCESC in vivo using NMRI fox1 nu/nu mouse tumor xenograft model. Mice were injected with MDA-MB-231 cells stably

transfected with the luciferase vector in the mammary fat pad. When the tumor became visible, mice were injected intraperitoneally, as described above, with DMEM-F12 (control), CM-hUCESC, paclitaxel or the combination of paclitaxel+CM-hUCESC. The evaluation of tumor growth could be analysed until day 21 because at day 28/30 many of the tumors showed necrosis. As it can be observed in Fig. 3, mice treated with paclitaxel showed a significantly reduction of the tumor growth compared with control (p < 0.0001; adjusted p value = 0.0007) and it was confirmed that the combination of chemotherapy treatment (paclitaxel) with the biological product (CM-hUCESC) significantly reduces tumor growth, especially at day 14 (p = 0.025; adjusted p value = 0.036). Although mice treated with CM-hUCESC showed less tumor growth than mice treated with paclitaxel+CM-hUCESC, there was no significant difference compared to the combination of treatments.

Effect of CM-hUCESC_{chemo} and its combination with paclitaxel

In order to improve the potential of CM-hUCESC and the effect of its combination with paclitaxel, hUCESC were cultured with a sublethal dose of chemotherapeutic prior to CM-hUCESC production. Subsequently, we evaluated the effect of CM-hUCESC_{chemo} and its combination on the proliferative and invasive capacity of MDA-MB-231, showing that it significantly decreased their functional capacities (Fig. 4A and B). CM-hUCESC_{chemo} decreased the proliferation of tumor cells (37.4%) similarly to paclitaxel (43.2%), but their combination showed a significant inhibition of proliferation by up to 86.4% (p < 0.0001; adjusted p value = 0.0007). Regarding the regulation of tumor cell invasiveness, the combination of paclitaxel with CM-hUCESC_{chemo} significantly decreased the capacity of cell invasion of tumor cells (compared with paclitaxel alone (p = 0.045; adjusted p value = 0.052)).

Characterization of CM-hUCESC_{chemo} extracellular vesicles

EVs and paclitaxel-loaded EVs were characterized by the following techniques. As can be seen in Fig. 4C, the presence of rounder vesicles in both samples was detected by Transmission Electron Microscopy (TEM). The paclitaxel-loaded EVs were slightly larger than the control EVs and the first ones possessed what it seemed like a lower electron density corona around them. For a better knowledge of the size distribution of the samples, Nanoparticle Tracking Analysis (NTA) analyses were performed. The size distribution graphs (Fig. 4D) also show an increase in size for paclitaxel-loaded EVs with a diameter media of 190 ± 8 nm and a mode of 132 ± 28 while control EVs have a diameter media of 130 ± 6 and a mode of 97 ± 14 nm. This is in agreement to previous studies: the EVs size increased proportionally to the amount of entrapped

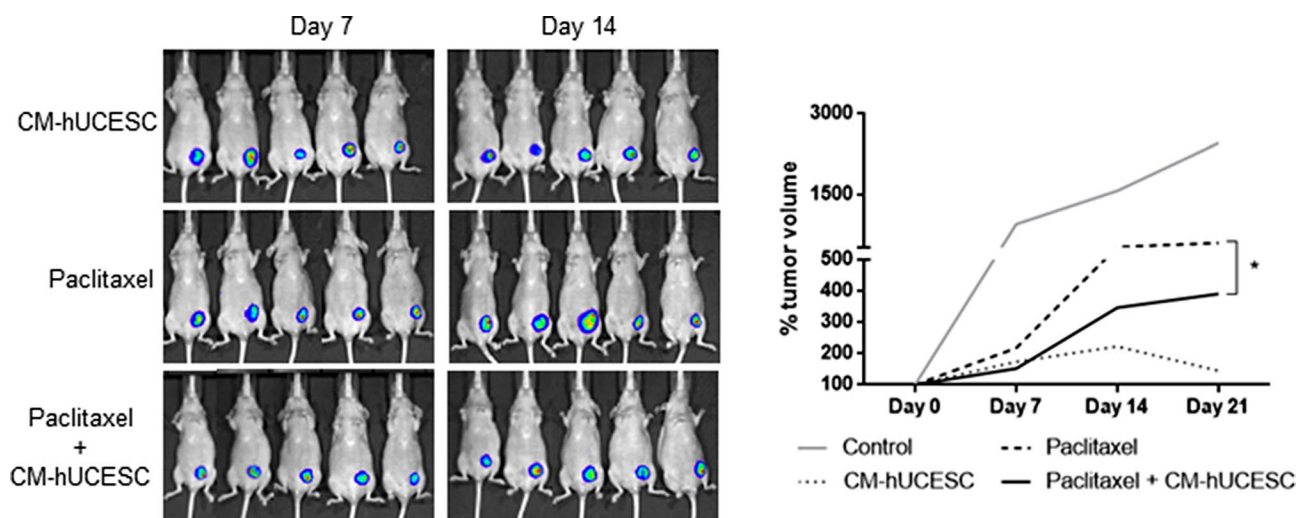


Fig. 3 Representative images from mice treated with CM-hUCESC, paclitaxel 10 mg/kg and the combination of paclitaxel 10 mg/kg + CM-hUCESC taken at 7 and 14 days and tumor volume which was determined by measuring luminescence since day 0 until day 21

drug [27, 28]. However, despite the differences in size, the control EVs and the paclitaxel-loaded EVs show the same markers (CD9, CD63 and CD81) (Supplementary Fig. 2). Regarding particle concentration calculated by NTA, an increase in particle production was observed for paclitaxel-treated cells ($1.34 \pm E11 \pm 0.21 + E11$ particles/mL vs. $0.47 \pm E11 \pm 0.03 + E11$ particles/mL for non-loaded EVs). This increase in particle production could be due to cellular stress produced by the paclitaxel treatment [23]. The bicinchoninic acid assay (BCA) also showed that this increase in particle concentration is correlated with a total protein rise (17.2 ± 1.6 vs. 14.4 ± 1.6 μ g/mL for paclitaxel-loaded EVs and control EVs, respectively).

Determination of paclitaxel in CM-hUCESC_{chemo}

Paclitaxel determination was performed in EVs and CM-hUCESC_{chemo} samples and hUCESC by HPLC-ESI-QTOF. Figure 4E and F show the Extracted Ion Chromatogram of paclitaxel ($m/z = 854.34 \pm 0.01$) for EV samples. As can be seen, paclitaxel was not detected in the control sample (Fig. 4E), but its presence is confirmed in the drug loaded vesicles (Fig. 4F).

Reducing tumor growth by combining CM-hUCESC_{chemo} with a lower dose of paclitaxel

Mice were injected intraperitoneally with DMEM-F12 (control), CM-hUCESC_{chemo}, paclitaxel or the combination of paclitaxel + CM-hUCESC_{chemo}. The evaluation of tumor growth could be analysed until day 21 because at day 28/30 many of the tumors showed necrosis. As it can be observed in Fig. 4G, mice treated with a low dose of paclitaxel (5 mg/kg) showed a similar tumor growth than control mice. Mice treated with CM-hUCESC_{chemo} showed a significant reduction of tumor growth, by almost of 60%, compared with paclitaxel alone (113%

vs. 274% tumor volume at day 14, respectively, $p = 0.032$; adjusted p value = 0.042), and by 20% compared with the combination of both treatment (113% vs. 131% tumor volume at day 14, respectively, no significant difference). However, the combination of paclitaxel (5 mg/kg) + CM-hUCESC_{chemo} showed a significant reduction, by almost of 50%, of tumor growth compared with paclitaxel alone (131% vs. 274% at day 14, respectively, $p = 0.016$; adjusted p value = 0.029), which means that a low dose of paclitaxel combined with CM-hUCESC can inhibit TNBC tumor growth in vivo.

Discussion

The results of the present study demonstrate the synergistic effect of the combination of CM-hUCESC with paclitaxel. First, the effect was evidenced in vitro through decreased cell proliferation and invasiveness of tumor cells and induction of apoptosis. Second, the effect was confirmed in a mouse tumor xenograft model showing that the combination of the chemotherapeutic agent with the secretome of hUCESC has a significant effect in reducing tumor growth. Third, pre-conditioning hUCESC with a sub-lethal dose of paclitaxel enhances the effect of its secretome and in combination with paclitaxel, even allows to reduce the dose of paclitaxel in vivo.

Controversial reports have been published regarding the pro- or anti-tumor effect of MSC [14, 29, 30], largely justified by the tissue of origin of MSC, the variability of stem cell donors and experimental conditions, among others [31, 32]. The source of MSC and the type of tumor seem to be the most influential factors in this controversy. In fact, many studies are contradictory regarding the effect on breast cancer cells of bone marrow (BM)-MSC and adipose tissue-derived (AD)-MSC or their derived-products [14]. However, relevant and consistent

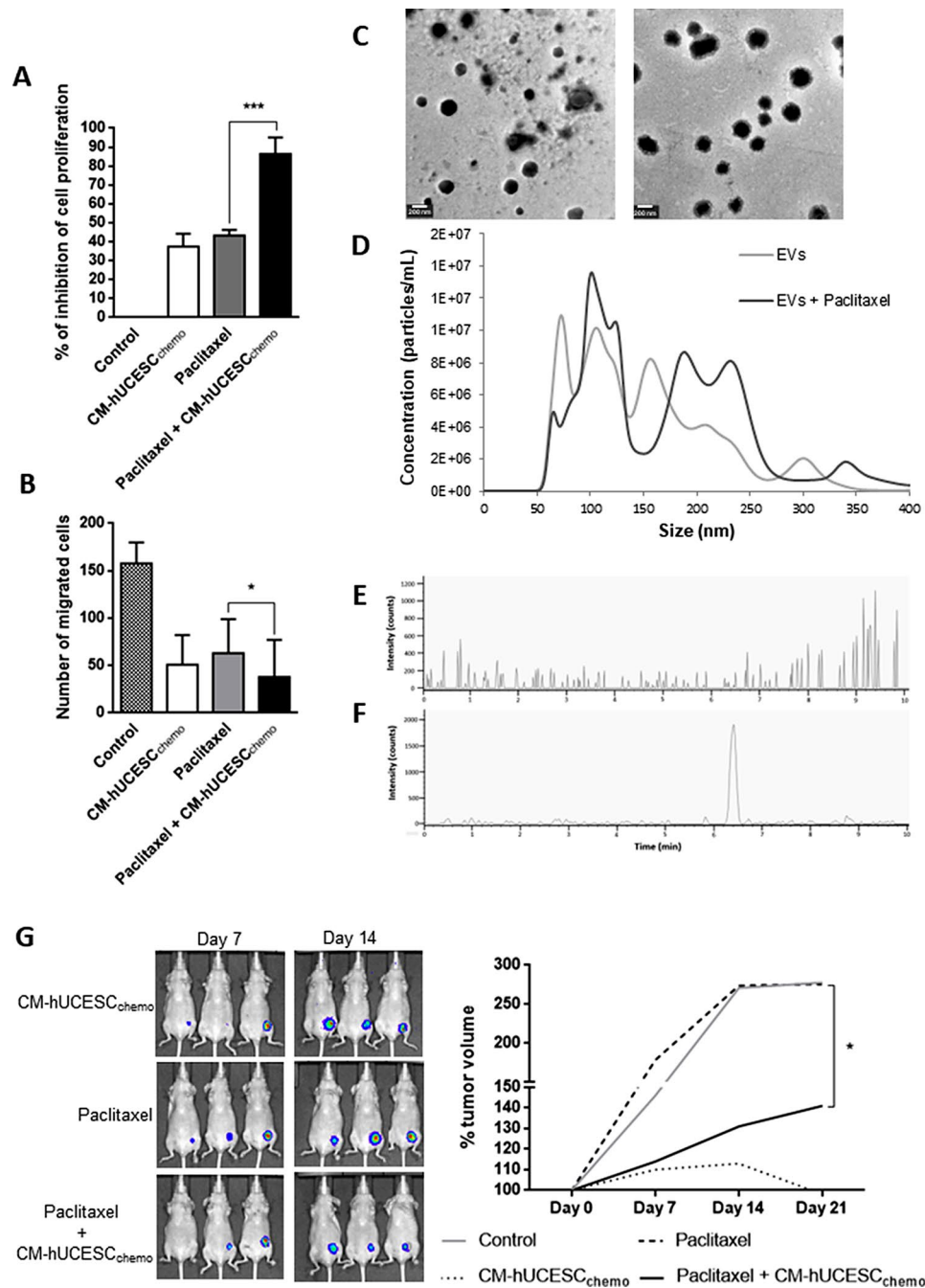


Fig. 4 **A**) Relative proliferative capacity of MDA-MB-231 cells treated with control (DMEM-F12 without FBS), CM-hUCESC_{chemo} (pre-conditioning of hUCESC with paclitaxel previously of CM production), paclitaxel (1 μ M) and the combination of paclitaxel (1 μ M)+CM-hUCESC_{chemo}. **B**) Invasive capacity of MDA-MB-231 cells treated with control (DMEM-F12 without FBS), CM-hUCESC_{chemo}, paclitaxel (1 μ M) and the combination of paclitaxel (1 μ M)+CM-hUCESC_{chemo}. **C**) Transmission Electron Microscopy micrographs for control EVs (left) and paclitaxel-loaded EVs (right). **D**) Size Distribution graphs by NTA for control EVs and drug loaded EVs. **E**) Extracted Ion Chromatogram by HPLC-ESI-TOF at paclitaxel mass/charge for control EVs. **F**) Extracted Ion Chromatogram by HPLC-ESI-TOF at paclitaxel mass/charge for drug-loaded EVs. **G**) Representative images from mice treated with CM-hUCESC_{chemo}, paclitaxel 5 mg/kg and the combination of paclitaxel 5 mg/kg+CM-hUCESC taken at 7 and 14 days and tumor volume which was determined by measuring luminescence since day 0 until day 21

results are found regarding the effect of MSC of uterine (i.e., cervix, endometrium) or reproductive tissue origin (i.e., umbilical cord) on breast and ovarian cancer cells, as shown by hUCESC previously [16, 33], as well as in the

present study through the effects on proliferation, apoptosis, and tumor-cell invasiveness. This leads to consider the importance of the tissue origin of MSC as it may influence their ability to regulate homeostasis in tissues

highly exposed to external aggressions such as the uterine cervix.

The MSC-derived secretome is composed of cytokines, growth factors and extracellular vesicles, among others, which represent a therapeutic alternative that avoids the drawbacks and offers solutions to the limitations associated with cell therapy, such as: (i) avoids transplantation of live and proliferative cells; (ii) offers similar safety assessment, dosage and potency to conventional pharmaceutical agents; (iii) offers easy storage; (iv) offers a more practical and cheaper clinical application; (v) allows the biological product obtained for therapeutic applications to be modified to suit the patient's needs, among others [26]. Other drawbacks of MSC cell therapy with regard to TNBC treatment have been reported, such as the immune rejection of the transplant due to repeated injections or prolonged exposure to MSC, leading to a poor MSC survival and function at the tumor site [15]. Although many research studies and clinical trials continue to approach cell therapy as an MSC-based therapy, more and more studies are being conducted based on the use of the secretome or cell-derived products [16, 33–37], as it is known that the mechanism of action of MSC is primarily paracrine.

Our results have shown that the secretome of hUCESC alone inhibits cell proliferation, induces apoptosis, regulates the cell cycle, and reduces the invasiveness of aggressive breast cancer cells, which differs from the results of the secretome of other types of MSC such as AD-MSC [38], but also potentiates these same effects of chemotherapy, unlike secretome of umbilical cord (UC)-MSC which did not significantly affect its cytotoxic, anti-migratory or anti-invasive effects on tumor cells [39]. Thus, the synergistic effect evidenced led us to investigate the impact of priming hUCESC with paclitaxel, before CM production, and its combination with chemotherapy on tumor cell behaviour. The use of a sublethal dose [23, 40] has allowed to potentiate the effect of paclitaxel *in vitro* and *in vivo*, but also to reduce the dose of paclitaxel administered to the mice, with a possible reduction of the side effects associated with the use of chemotherapy.

The observed effects could be partly due to the incorporation of paclitaxel into the extracellular vesicles released into the environment by the hUCESC, since the presence of paclitaxel in the EVs present in the CM-hUCESC_{chemo} has been observed. The incorporation of paclitaxel into EVs produced an increase in particle size and number, probably due to cellular stress induced by the paclitaxel treatment. Most of EVs present in this CM-hUCESC can be classified into exosomes by size (30–150 nm). These EVs are of great interest as a possible alternative to exploiting the properties of MSC, or at least part of them, due to their advantages such as better safety profile, lower immunogenicity, the ability

to cross biological barriers (gastrointestinal barrier and blood–brain barrier), and to avoid immune rejection [14, 41–43]. EVs are one of the interaction pathways between MSC and breast cancer tumor cells, MSC-derived EVs (MSC-EVs) can transport molecules, such as proteins and nucleic acids, through which they exert inhibitory or promoter effects on breast cancer cells [13, 44]. At the same time, MSC-EVs provide new therapeutic options such as being carriers for drug delivery [45]. Indeed, other studies demonstrated the therapeutic efficacy of either paclitaxel-loaded MSC-CM [46] or -EVs [47, 48] and even that paclitaxel incorporated into MSC-EVs induced the same effects at a reduced concentration as the direct use of the chemotherapeutic agent, indicating that chemotherapeutic-loaded MSC-Es have a specific and more efficient property to attack tumors [23], due to the internalisation of EVs by target cells. The loading process can be enhanced by electroporation, lipofection, sonication or extrusion [49], instead of use a passive incorporation, as genuinely appear to display the hUCESC. Therefore, our study is in the current research line that point to the special interest of CM and EVs derived from MSC for the treatment of TNBC [48, 50–52].

There are other mechanisms that could explain the anti-tumor effect induced by CM-hUCESC. Thus, for example, the involvement of matrix metalloproteinases (MMPs) in cancer progression through the processes of cell migration and invasion has been widely reported [53–57]. The activity of MMPs is controlled by tissue inhibitors of metalloproteinases (TIMPs) to prevent excessive proteolysis, tissue damage, migration and invasion of tumor cells through basement membrane degradation. Of fact, it has been reported that the anti-tumor effect of MSC may be partly related to the activity of the TIMP-1 and TIMP-2 [58]. A previous proteomic study has revealed the presence of high levels of TIMP-1 and TIMP-2 in CM-hUCESC [59], and in the present study we have evidenced that these factor secreted by hUCESC contribute to the regulation of tumor aggressiveness through the inhibition of tumor cell invasion, as well as being implicated in other non-tumor processes induced by CM-hUCESC [24].

In summary, this study on CM-hUCESC provided several novelties, such as (i) the combination of the biological product CM-hUCESC with chemotherapy (Paclitaxel); (ii) the demonstration of the effect of this combination, *in vitro*, on cell proliferation, invasiveness and apoptosis of breast cancer tumor cells (MDA-MB-231 and/or primary tumor cells); (iii) the anti-tumor effect was confirmed in a mouse tumor xenograft model showing that the combination of both products has a significant effect in reducing tumor growth; (iv) pre-conditioning hUCESC with a sub-lethal dose of paclitaxel enhances the effect of its secretome, *in vitro* and *in vivo*; (v) the combination of the

secretome from pre-conditioned hUCESC with paclitaxel reduced significantly tumor growth and even allows to diminish the dose of paclitaxel, *in vivo*; (vi) mechanism of action based on soluble factors present in the secretome, such as TIMP-1 and TIMP-2, and extracellular vesicles (EVs).

Conclusions

In conclusion, our data indicate that CM-hUCESC enhances the chemotherapy effects on triple negative breast cancer cells and opens an opportunity to reduce the dose of the chemotherapeutic agents, which may decrease chemotherapy-related toxicity. This effect is in part due to the action of their EVs and soluble factors, such as TIMP-1 and -2. In addition, the possibility to obtain EVs loaded with chemotherapeutic agents open the scenario for more selective anti-tumor strategies. We consider that our study also suggests the interest of future studies on the mechanisms underlying, such as PI3K/AKT/NFκB pathway and on the tropism of the MSC derived-EVs toward tumors, as well as to explore the possible impact of CM-hUCESC to relieve chemotherapy-induced tissue injuries, such as cardiotoxicity, nephrotoxicity, pulmonary toxicity, and reproductive tract toxicity.

Abbreviations

(AD)-MSC	adipose tissue-derived mesenchymal stem cells
(BM)-MSC	bone marrow mesenchymal stem cells
CM-hUCESC	secretome derived from human Uterine Cervical Stem cells
ER	estrogen receptor
EVs	extracellular vesicles
HER-2	human epidermal growth factor receptor 2
hUCESC	human Uterine Cervical Stem Cells
MMPs	matrix metalloproteinases
MSC	mesenchymal stem cells
PD-L1	PD-L1
PR	progesterone
TEM	Transmission Electron Microscopy
TIMPs	tissue inhibitors of metalloproteinases
TNBC	triple-negative breast cancer

Supplementary Information

The online version contains supplementary material available at <https://doi.org/10.1186/s13287-024-03717-0>.

Supplementary Material 1

Supplementary Material 2

Acknowledgements

Not applicable.

Authors' contributions

Conceptualization, N.E. and F.J.V.; methodology, N.E., M.F., S.E.-C., J.S.-L., M.L.F.-S. and L.O.G.; formal analysis, N.E., M.F. and F.J.V.; investigation, N.E., M.F., S.E.-C., J.S.-L. and L.O.G.; writing—original draft preparation, N.E., M.F., and F.J.V.; writing—review and editing, N.E., M.F., S.E.-C., J.S.-L., L.O.G., M.L.F.-S. and F.J.V.; project administration, N.E. and F.J.V.; funding acquisition, N.E. and F.J.V. All authors have read and agreed to the published version of the manuscript.

Funding

This study was supported by grants from Instituto de Salud Carlos III, grant number PI17/02236 to F.J.V. and PI20/01122 to N.E. and F.J.V., and co-funded by European Union (ERDF/ESF, "Investing in your future"). Grants to M.L.S.-F from the Principality of Asturias (GRUPIN IDI 2021/000081) and the Spanish Ministry of Science and Innovation (PID2022-142323NB-I00), funded by MCIN/AEI/10.13039/501100011033/ and by "ERDF A way of making Europe, provided funding for part of this work. S.E.-C thanks the Principality of Asturias for the Severo Ochoa grant (PA-21-PF-BP20-067). The funding body played no role in the design of the study and collection, analysis, and interpretation of data and in writing the manuscript.

Data availability

The data presented in this study are available on request from the corresponding author.

Declarations

Ethical approval

All human specimens were encoded to protect patient confidentiality and processed under protocols approved by the regional Ethics and Investigation Committee (Comité Ético de Investigación Clínica Regional del Principado de Asturias). Women were treated according to the guidelines used in our Institution (Fundación Hospital de Jove). Written informed consent was obtained from all donors. The study adhered to National regulations and was approved by Ethical Committee of Regional Clinical Research of the Principality of Asturias (title: Evaluation of a new therapeutic strategy for triple negative breast cancer and ovary epithelial cancer based on the secretome of mesenchymal stem cells from the uterine cervix; ref: 99/18, 21 March 2018). The animal studies were conducted according to the ARRIVE guidelines (Animal Research: Reporting of In Vivo Experiments) and approved by the Universidad de Santiago de Compostela Ethics Committee for Animal Experiments (Project title: Breast cancer: tumor cell and stroma as therapeutic targets of stem cells and vitamin D analogues. Approval no: 15010/16/001, March 2, 2016).

Competing interests

The authors declare no conflict of interest. N.E. and F.J.V. are co-inventors of a patent ("Human uterine cervical stem cell population and uses thereof") owned by GiStem Research, of which some authors are shareholders (N.E., J.S.-L., L.O.G., M.L.F.-S. and F.J.V.). The founding sponsors had no role in the design of this manuscript, in the collection, analyses, or interpretation of data, in the writing of the manuscript, or in the decision to publish the results.

Received: 1 September 2023 / Accepted: 7 April 2024

Published online: 25 April 2024

References

1. Hajdu SI. A note from history: landmarks in history of cancer, part 1. *Cancer*. 2011;117(5):1097–102.
2. DeVita VT Jr, Chu E. A history of cancer chemotherapy. *Cancer Res*. 2008;68(21):8643–53.
3. Wani MC, Taylor HL, Wall ME, Coggon P, McPhail AT. Plant Antitumor agents. VI. The isolation and structure of taxol, a novel antileukemic and antitumor agent from *Taxus brevifolia*. *J Am Chem Soc*. 1971;93(9):2325–7.
4. Schirmacher V. From chemotherapy to biological therapy: a review of novel concepts to reduce the side effects of systemic cancer treatment (review). *Int J Oncol*. 2019;54(2):407–19.
5. Azim HA Jr, de Azambuja E, Colozza M, Bines J, Piccart MJ. Long-term toxic effects of adjuvant chemotherapy in breast cancer. *Ann Oncol*. 2011;22(9):1939–47.
6. Rattanakrong N, Siriphorn A, Boonyong S. Incidence density and factors associated with peripheral neuropathy among women with breast cancer during taxane-based chemotherapy. *Sci Rep*. 2022;12(1):10632.
7. Manjunath M, Choudhary B. Triple-negative breast cancer: a run-through of features, classification and current therapies. *Oncol Lett*. 2021;22(1):512.
8. Sung H, Ferlay J, Siegel RL, Laversanne M, Soerjomataram I, Jemal A, et al. Global Cancer statistics 2020: GLOBOCAN estimates of incidence and

- Mortality Worldwide for 36 cancers in 185 countries. *CA Cancer J Clin.* 2021;71(3):209–49.
9. Howlander N, Cronin KA, Kurian AW, Andridge R. Differences in breast Cancer survival by Molecular subtypes in the United States. *Cancer Epidemiol Biomarkers Prev.* 2018;27(6):619–26.
 10. Debien V, De Caluwe A, Wang X, Piccart-Gebhart M, Tuohy VK, Romano E, et al. Immunotherapy in breast cancer: an overview of current strategies and perspectives. *NPJ Breast Cancer.* 2023;9(1):7.
 11. Loizides S, Constantinidou A. Triple negative breast cancer: immunogenicity, tumor microenvironment, and immunotherapy. *Front Genet.* 2022;13:1095839.
 12. Dominici M, Le Blanc K, Mueller I, Slaper-Cortenbach I, Marini F, Krause D, et al. Minimal criteria for defining multipotent mesenchymal stromal cells. The International Society for Cellular Therapy position statement. *Cytotherapy.* 2006;8(4):315–7.
 13. Fernandez-Francos S, Eiro N, Costa LA, Escudero-Cernuda S, Fernandez-Sanchez ML, Vizoso FJ. Mesenchymal Stem Cells as a Cornerstone in a Galaxy of InterCellular Signals: Basis for a New Era of Medicine. *Int J Mol Sci.* 2021;22(7).
 14. Eiro N, Fraile M, Fernandez-Francos S, Sanchez R, Costa LA, Vizoso FJ. Importance of the origin of mesenchymal (stem) stromal cells in cancer biology: alliance or war in intercellular signals. *Cell Biosci.* 2021;11(1):109.
 15. Wu Y, Shum HCE, Wu K, Vadgama J. From Interaction to intervention: how mesenchymal stem cells affect and target triple-negative breast Cancer. *Biomedicines.* 2023;11(4).
 16. Eiro N, Sendon-Lago J, Seoane S, Bermudez MA, Lamelas ML, Garcia-Caballero T, et al. Potential therapeutic effect of the secretome from human uterine cervical stem cells against both cancer and stromal cells compared with adipose tissue stem cells. *Oncotarget.* 2014;5(21):10692–708.
 17. Schneider J, Eiro N, Perez-Fernandez R, Martinez-Ordonez A, Vizoso F. Human uterine cervical stromal stem cells (hUCESCs): why and how they exert their Antitumor activity. *Cancer Genomics Proteom.* 2016;13(5):331–7.
 18. Karnoub AE, Dash AB, Vo AP, Sullivan A, Brooks MW, Bell GW, et al. Mesenchymal stem cells within tumour stroma promote breast cancer metastasis. *Nature.* 2007;449(7162):557–63.
 19. Muehlberg FL, Song YH, Krohn A, Pinilla SP, Droll LH, Leng X, et al. Tissue-resident stem cells promote breast cancer growth and metastasis. *Carcinogenesis.* 2009;30(4):589–97.
 20. Galie M, Konstantinidou G, Peroni D, Scambi I, Marchini C, Lisi V, et al. Mesenchymal stem cells share molecular signature with mesenchymal tumor cells and favor early tumor growth in syngeneic mice. *Oncogene.* 2008;27(18):2542–51.
 21. Eiro N, Gonzalez L, Martinez-Ordonez A, Fernandez-Garcia B, Gonzalez LO, Cid S, et al. Cancer-associated fibroblasts affect breast cancer cell gene expression, invasion and angiogenesis. *Cell Oncol (Dordr).* 2018;41(4):369–78.
 22. Eiro N, Cid S, Aguado N, Fraile M, de Pablo N, Fernandez B et al. MMP1 and MMP11 expression in Peripheral Blood mononuclear cells upon their interaction with breast Cancer cells and fibroblasts. *Int J Mol Sci.* 2020;22(1).
 23. Melzer C, Rehn V, Yang Y, Bahre H, von der Ohe J, Hass R. Taxol-loaded MSC-Derived exosomes provide a therapeutic vehicle to target metastatic breast Cancer and other Carcinoma cells. *Cancers (Basel).* 2019;11(6).
 24. Sendon-Lago J, Seoane S, Martinez-Ordonez A, Eiro N, Saa J, Vizoso FJ, et al. Corneal regeneration by conditioned medium of human uterine cervical stem cells is mediated by TIMP-1 and TIMP-2. *Exp Eye Res.* 2019;180:110–21.
 25. Li P, Kaslan M, Lee SH, Yao J, Gao Z. Progress Exosome Isolation Techniques Theranostics. 2017;7(3):789–804.
 26. Vizoso FJ, Eiro N, Cid S, Schneider J, Perez-Fernandez R. Mesenchymal stem cell secretome: toward cell-free therapeutic strategies in Regenerative Medicine. *Int J Mol Sci.* 2017;18(9).
 27. Kim MS, Haney MJ, Zhao Y, Mahajan V, Deygen I, Klyachko NL, et al. Development of exosome-encapsulated paclitaxel to overcome MDR in cancer cells. *Nanomedicine.* 2016;12(3):655–64.
 28. Salarpour S, Forooutanfar H, Pournamdari M, Ahmadi-Zeidabadi M, Esmaeili M, Pardakhty A. Paclitaxel incorporated exosomes derived from glioblastoma cells: comparative study of two loading techniques. *Daru.* 2019;27(2):533–9.
 29. Rhee KJ, Lee JI, Eom YW. Mesenchymal stem cell-mediated effects of Tumor support or suppression. *Int J Mol Sci.* 2015;16(12):30015–33.
 30. Hmadcha A, Martin-Montalvo A, Gauthier BR, Soria B, Capilla-Gonzalez V. Therapeutic potential of mesenchymal stem cells for Cancer Therapy. *Front Bioeng Biotechnol.* 2020;8:43.
 31. Heidari R, Gholamian Dehkordi N, Mohseni R, Safaei M. Engineering mesenchymal stem cells: a novel therapeutic approach in breast cancer. *J Drug Target.* 2020;28(7–8):732–41.
 32. Costa LA, Eiro N, Fraile M, Gonzalez LO, Saa J, Garcia-Portabella P, et al. Functional heterogeneity of mesenchymal stem cells from natural niches to culture conditions: implications for further clinical uses. *Cell Mol Life Sci.* 2021;78(2):447–67.
 33. Sendon-Lago J, Seoane S, Saleh F, Garcia-Caballero L, Arias ME, Eiro N, et al. In vivo effects of conditioned medium from human uterine cervical stem cells in an ovarian Cancer Xenograft Mouse Model. *Cancer Genomics Proteom.* 2022;19(5):570–5.
 34. Nadesh R, Menon KN, Biswas L, Mony U, Subramania Iyer K, Vijayaraghavan S, et al. Adipose derived mesenchymal stem cell secretome formulation as a biotherapeutic to inhibit growth of drug resistant triple negative breast cancer. *Sci Rep.* 2021;11(1):23435.
 35. Serras AS, Camões SP, Antunes B, Costa VM, Dionisio F, Yazar V et al. The Secretome of Human neonatal mesenchymal stem cells modulates Doxorubicin-Induced cytotoxicity: impact in Non-tumor cells. *Int J Mol Sci.* 2021;22(23).
 36. Sousa A, Coelho P, Leite F, Teixeira C, Rocha AC, Santos I et al. Impact of umbilical cord mesenchymal stromal/stem cell secretome and cord blood serum in prostate cancer progression. *Hum Cell.* 2023.
 37. Han KH, Kim AK, Jeong GJ, Jeon HR, Bhang SH, Kim DI. Enhanced Anti-cancer effects of Conditioned Medium from Hypoxic Human umbilical cord-derived mesenchymal stem cells. *Int J Stem Cells.* 2019;12(2):291–303.
 38. de Miranda MC, Ferreira ADF, de Melo MIA, Kunrath-Lima M, Goes AM, Rodrigues MA, et al. Adipose-derived stem/stromal cell secretome modulates breast cancer cell proliferation and differentiation state towards aggressiveness. *Biochimie.* 2021;191:69–77.
 39. Serras AS, Camoes SP, Antunes B, Costa VM, Dionisio F, Yazar V et al. The Secretome of Human neonatal mesenchymal stem cells modulates Doxorubicin-Induced cytotoxicity: impact in Non-tumor cells. *Int J Mol Sci.* 2021;22(23).
 40. Bosco DB, Kenworthy R, Zorio DA, Sang QX. Human mesenchymal stem cells are resistant to Paclitaxel by adopting a non-proliferative fibroblastic state. *PLoS ONE.* 2015;10(6):e0128511.
 41. Witwer KW, Van Balkom BWM, Bruno S, Choo A, Dominici M, Gimona M, et al. Defining mesenchymal stromal cell (MSC)-derived small extracellular vesicles for therapeutic applications. *J Extracell Vesicles.* 2019;8(1):1609206.
 42. Kou M, Huang L, Yang J, Chiang Z, Chen S, Liu J, et al. Mesenchymal stem cell-derived extracellular vesicles for immunomodulation and regeneration: a next generation therapeutic tool? *Cell Death Dis.* 2022;13(7):580.
 43. Harrell CR, Jovicic N, Djonov V, Arsenijevic N, Volarevic V. Mesenchymal stem cell-derived exosomes and other Extracellular vesicles as new remedies in the Therapy of Inflammatory diseases. *Cells.* 2019;8(12).
 44. Guo Y, Zhai Y, Wu L, Wang Y, Wu P, Xiong L. Mesenchymal stem cell-derived extracellular vesicles: pleiotropic impacts on breast Cancer occurrence, Development, and Therapy. *Int J Mol Sci.* 2022;23(6).
 45. Lin Y, Lu Y, Li X. Biological characteristics of exosomes and genetically engineered exosomes for the targeted delivery of therapeutic agents. *J Drug Target.* 2020;28(2):129–41.
 46. Cordani N, Lisini D, Coccè V, Paglia G, Meanti R, Cerrito MG et al. Conditioned medium of mesenchymal stromal cells loaded with paclitaxel is effective in Preclinical models of Triple-negative breast Cancer (TNBC). *Int J Mol Sci.* 2023;24(6).
 47. Kalimuthu S, Gangadaran P, Rajendran RL, Zhu L, Oh JM, Lee HW, et al. A New Approach for Loading Anticancer drugs into mesenchymal stem cell-derived Exosome Mimetics for Cancer Therapy. *Front Pharmacol.* 2018;9:1116.
 48. Basak M, Sahoo B, Chaudhary DK, Narisepalli S, Tiwari S, Chitkara D, et al. Human umbilical cord blood-mesenchymal stem cell derived exosomes as an efficient nanocarrier for Docetaxel and miR-125a: Formulation optimization and anti-metastatic behaviour. *Life Sci.* 2023;322:121621.
 49. Peng H, Ji W, Zhao R, Yang J, Lu Z, Li Y, et al. Exosome: a significant nano-scale drug delivery carrier. *J Mater Chem B.* 2020;8(34):7591–608.
 50. Shojaei S, Hashemi SM, Ghanbarian H, Sharifi K, Salehi M, Mohammadi-Yeganeh S. Delivery of mir-381-3p mimic by mesenchymal stem cell-derived Exosomes inhibits Triple negative breast Cancer aggressiveness; an in Vitro Study. *Stem Cell Rev Rep.* 2021;17(3):1027–38.
 51. Khazaei-Poul Y, Shojaei S, Koochaki A, Ghanbarian H, Mohammadi-Yeganeh S. Evaluating the influence of human umbilical cord mesenchymal stem cells-derived exosomes loaded with miR-3182 on metastatic performance of Triple negative breast Cancer cells. *Life Sci.* 2021;286:120015.
 52. Farhadi S, Mohammadi-Yeganeh S, Kiani J, Hashemi SM, Koochaki A, Sharifi K, et al. Exosomal delivery of 7SK long non-coding RNA suppresses viability, proliferation, aggressiveness and tumorigenicity in triple negative breast cancer cells. *Life Sci.* 2023;322:121646.

53. Menyhart O, Harami-Papp H, Sukumar S, Schafer R, Magnani L, de Barrios O, et al. Guidelines for the selection of functional assays to evaluate the hallmarks of cancer. *Biochim Biophys Acta*. 2016;1866(2):300–19.
54. Eiro N, Gonzalez LO, Fraile M, Cid S, Schneider J, Vizoso FJ. Breast Cancer Tumor Stroma: Cellular Components, phenotypic heterogeneity, Intercellular Communication, Prognostic implications and Therapeutic opportunities. *Cancers (Basel)*. 2019;11(5).
55. Eiró N, Fernandez-Garcia B, Vázquez J, Del Casar JM, González LO, Vizoso FJ. A phenotype from tumor stroma based on the expression of metalloproteases and their inhibitors, associated with prognosis in breast cancer. *Oncoimmunology*. 2015;4(7):e992222.
56. Eiro N, Cid S, Aguado N, Fraile M, de Pablo N, Fernández B et al. MMP1 and MMP11 expression in Peripheral Blood mononuclear cells upon their Interaction with breast Cancer cells and fibroblasts. *Int J Mol Sci*. 2020;22(1).
57. Eiro N, Cid S, Fernandez B, Fraile M, Cernea A, Sanchez R, et al. MMP11 expression in intratumoral inflammatory cells in breast cancer. *Histopathology*. 2019;75(6):916–30.
58. Lozito TP, Tuan RS. Mesenchymal stem cells inhibit both endogenous and exogenous MMPs via secreted TIMPs. *J Cell Physiol*. 2011;226(2):385–96.
59. Bermudez MA, Sendon-Lago J, Eiro N, Trevino M, Gonzalez F, Yebra-Pimentel E, et al. Corneal epithelial wound healing and bactericidal effect of conditioned medium from human uterine cervical stem cells. *Invest Ophthalmol Vis Sci*. 2015;56(2):983–92.

Publisher's Note

Springer Nature remains neutral with regard to jurisdictional claims in published maps and institutional affiliations.